

# Microstructure Characterisation and Oxygen Sensing Properties of $\text{Al}_2\text{O}_3\text{-ZrO}_2\text{-Y}_2\text{O}_3$ Shaped Eutectic Composites

Serge Zhuiykov\*

Department of Communication and Electronic Engineering, RMIT University,  
GPO Box 2476V, Melbourne, VIC. 3001, Australia

(Received November 29, 1999; accepted June 22, 2000)

**Key words:** eutectic composites, microstructure, oxygen sensors, alumina-ytria-zirconia

Shaped cylindrical eutectic  $\text{Al}_2\text{O}_3\text{-ZrO}_2\text{-Y}_2\text{O}_3$  composites were grown by the Stepanov technique. The morphology, crystalline structure and chemical composition of the  $\text{Al}_2\text{O}_3\text{-ZrO}_2\text{-Y}_2\text{O}_3$  samples were investigated using scanning electronic microscopy (SEM) and X-ray photoelectron spectroscopy (XPS). Specimens were highly pure with carbon as the dominant impurity at the surface. The  $\text{Al}_2\text{O}_3\text{-ZrO}_2\text{-Y}_2\text{O}_3$  composites have also been employed as solid electrolytes in oxygen sensors. The main characteristics and performance of the  $\text{Al}_2\text{O}_3\text{-ZrO}_2\text{-Y}_2\text{O}_3$  composites in oxygen sensors were investigated by electrochemical methods at an operating temperature range of 400 to 1000°C. The electromotive force (EMF) response of each sensor closely followed the Nernst equation. The  $\text{Al}_2\text{O}_3\text{-ZrO}_2\text{-Y}_2\text{O}_3$  eutectic composites with Pt electrodes behave as pure ionic conductors in the oxygen sensors at operating temperatures as low as 480°C.

## 1. Introduction

Research on new ionic composite materials based on stabilised fluorite structures still attracts the interest of scientists. The research concentrates mainly on obtaining incremental improvements in the properties of these composites. Any increases in the conductivity at low temperature are important in terms of enhancing the efficiency of systems such as oxygen sensors. Moreover, any reduction in the operating temperature of the oxygen sensor by the manufacturing technology has a considerable effect on materials selection

---

\*Present address: Advanced Science & Technology Centre for Cooperative Research, Kyushu University, Kasuga-shi, Fukuoka 816-8580, Japan. e-mail: serge@astec.kyushu-u.ac.jp

and lifetime predictions for such devices.<sup>(1)</sup> In the search for new manufacturing technologies for solid electrolyte systems with pure ionic conductivity, parameters such as high strength, chemical stability with respect to other sensor components, cost of materials and specialised processing conditions must not be ignored if such materials are to be of practical use in commercial devices.<sup>(1-4)</sup> The technology of growing of eutectic composites is very promising for solid electrolyte materials. From a practical point of view, the development of stable solid electrolytes with pure ionic conductivity at both low and high temperatures is required to achieve more versatile measuring instruments. Due to the steady increase in electronic conductivity of the  $\text{ZrO}_2\text{-Y}_2\text{O}_3$  solid electrolytes at temperatures lower than  $700^\circ\text{C}$ , few attempts have been made to find the best solid electrolytes for oxygen sensors which are capable of functioning reliably at temperatures from  $400^\circ$  to  $700^\circ\text{C}$ .<sup>(4-6)</sup>

Solid electrolytes based on the  $\text{ZrO}_2\text{-Sc}_2\text{O}_3$  system are of considerable interest as candidate materials for intermediate temperature oxygen sensors because these systems have the highest conductivity of any known zirconia stabilised electrolytes.<sup>(7)</sup> However,  $\text{Sc}_2\text{O}_3$  as a material is still relatively expensive. Furthermore, the deterioration of the conductivity of  $\text{ZrO}_2\text{-Sc}_2\text{O}_3$  systems is another factor limiting the widespread application of this solid electrolyte in oxygen sensors.

During the last decade, improvements in sensor design have led to a substantial shift of the threshold temperature of operation towards a lower temperature, where a significant output EMF can be obtained. However, the lowest working temperature of zirconia sensors is restricted by impurities in stabilised zirconia which affect its electronic conductivity.<sup>(8,9)</sup> Therefore, in most sensor applications, the electronic conductivity of zirconia should be lower than the ionic conductivity by more than three orders of magnitude.<sup>(9)</sup> Although accurate oxygen sensors with operating temperatures lower than  $600^\circ\text{C}$  are needed, the electronic conductivity has a significant influence on the total conductivity of polycrystalline zirconia at temperatures below  $600^\circ\text{C}$ . Several investigations have appeared recently<sup>(10-12)</sup> providing detailed information on various aspects of decreasing the influence of electronic conductivity of polycrystalline zirconia at low temperatures. Previous analytical work<sup>(10)</sup> supplied a great deal of valuable information on different aspects of using the tetragonal phase of 3 mol% yttria-doped zirconia for low temperature sensors. Though the ionic conductivity is smaller than that of 8 mol% yttria-doped zirconia, handling is easier during the sensor fabrication process. The problem associated with this material is the chemical stability. The ionic conductivity degrades during long term operation. Grain boundary segregation as well as the formation of monoclinic phase may be the reason for the degradation.<sup>(9)</sup> In addition, the surface of zirconia in these sensors is given a hydrofluoric acid treatment before the Pt electrodes are applied. This treatment reduces polarisation of the electrodes and allows accurate oxygen measurement at the comparatively lower temperature of  $400^\circ\text{C}$ .

Among other solid electrolyte oxygen sensors for low and intermediate temperature measurements, the sensor based on a zirconia single crystal in combination with molten metal-metal oxide reference electrodes and with a  $\text{Pt-ZrO}_2\text{-Y}_2\text{O}_3$  thin-film measuring electrode<sup>(13)</sup> was the most effective for accurate oxygen measurements at temperatures as low as  $360\text{--}600^\circ\text{C}$ . This appears to indicate that the oxygen sensor based on zirconia single crystal is a serious contender for other low-temperature oxygen sensors based on polycrys-

talline zirconia. However, due to the high cost of single crystal growth and the complex manufacturing technology of these sensors, the development of alternative, inexpensive but pure ionic conductors for low-temperature oxygen sensors with good ceramic properties is still in demand.

More recently, the growth of  $\text{Al}_2\text{O}_3\text{-ZrO}_2(\text{Y}_2\text{O}_3)$  eutectic composites by the Stepanov technique and preliminary data on the mechanical properties and crystal structure have been reported.<sup>(14)</sup> The chemical resistance of zirconia eutectic composites is three times higher than the conventional polycrystalline zirconia electrolytes.<sup>(14)</sup> Therefore, oxide-oxide solid electrolyte eutectic composites were considered as potential materials for low-temperature oxygen sensors. In these eutectic composites the negative influence of impurities segregation on the grain boundaries of zirconia is minimised. This is due to the single crystal nature of the zirconia fibres in the  $\text{Al}_2\text{O}_3\text{-ZrO}_2(\text{Y}_2\text{O}_3)$  composites. Consequently, the contribution of electronic conductivity to the total conductivity of the solid electrolyte could be decreased. This study deals with a detailed investigation of the microstructure and characteristics of oxygen sensors based on  $\text{Al}_2\text{O}_3\text{-ZrO}_2(\text{Y}_2\text{O}_3)$ -shaped cylindrical eutectic composites.

## 2. Experimental Procedure

### 2.1 Sample preparation

All samples of  $\text{Al}_2\text{O}_3\text{-ZrO}_2\text{-Y}_2\text{O}_3$  composites used in this study were prepared from high purity (99.99%) powders of alumina, zirconia and yttria. These powders were calcined, weighed in the desired proportions (49.9 wt%  $\text{Al}_2\text{O}_3$ , 45.7 wt%  $\text{ZrO}_2$  and 4.4 wt%  $\text{Y}_2\text{O}_3$ ) and mixed. Cylinders of the  $\text{Al}_2\text{O}_3\text{-ZrO}_2\text{-Y}_2\text{O}_3$  eutectic composites were grown by the Stepanov technique in a resistance-heated furnace ( $\sim 2000^\circ\text{C}$ , vacuum  $\sim 10^{-5}$  Torr) equipped with a graphite heater and afterheaters using an argon atmosphere at pressures of 1.1–1.5 atm. Molybdenum crucibles and die were used. The die was a cylindrical ring tightly packed with molybdenum wires 0.35 mm in diameter. Rod-shaped  $\text{Al}_2\text{O}_3\text{-ZrO}_2\text{-Y}_2\text{O}_3$  composites 5–7 mm in diameter were grown in ROSTOX-N Ltd. (Russia) in lengths up to 300 mm. Sapphire bars  $3 \times 3 \times 40$  mm in size were used as seed crystals. The growth rates were 20–100 mm/h. Samples were cut, polished and finished with diamond paste.

The polycrystalline  $\text{Al}_2\text{O}_3\text{-ZrO}_2\text{-Y}_2\text{O}_3$  solid electrolyte (49.9 wt%  $\text{Al}_2\text{O}_3$ , 45.7 wt%  $\text{ZrO}_2$  and 4.4 wt%  $\text{Y}_2\text{O}_3$ ) were also made from high purity (99.99%) powders of alumina, zirconia and yttria. The cylindrical specimens 6 mm in diameter were sintered at  $1650^\circ\text{C}$  for two hours.

Finally, both  $\text{Al}_2\text{O}_3\text{-ZrO}_2\text{-Y}_2\text{O}_3$  eutectic composites and polycrystalline  $\text{Al}_2\text{O}_3\text{-ZrO}_2\text{-Y}_2\text{O}_3$  cylinders with lengths lower than 10 mm were assembled into a leak-proof alumina insulating tube. A technique developed in the CSIRO, Division of Materials Science (Australia) was used for this purpose. This technique involves joining a solid electrolyte pellet or cylinder to an alumina tube of the required length and diameter by a high temperature eutectic welding operation.<sup>(15)</sup> The sensors thus prepared are rugged in construction, have low leak rate and are suitable for most industrial and laboratory applications. The cylinder-tube design of the oxygen sensor is a robust form of construction and avoids any possible leaks through the junction of the eutectic composite and

insulating tube.<sup>(16)</sup> Both measuring and reference electrodes were made by applying Pt paste on the composite. A built-in K-type thermocouple was used.

## 2.2 Microstructure characterisation and gas sensing properties

Subsequently, the microstructure and the surface topography of the  $\text{Al}_2\text{O}_3\text{-ZrO}_2\text{-Y}_2\text{O}_3$  specimens were examined using a field emission scanning electron microscope JEOL JSM-6440F fitted with both a digital imaging system for electron microscopy and an energy dispersive X-ray detector VOYAGER at Kyushu University (Japan). Specimens of the eutectic crystals were polished by using Metadi II-diamond polishing compound (USA) and were coated with a 30-nm-thick coating of carbon.

The chemical composition of the specimens was examined using XPS on a VG Microlab 310F at RMIT University (Australia). An Al anode unmonochromated X-ray source operated at a power of 300 W and 15 kV excitation voltage was used. The energy of the Al  $K\alpha$  line was taken to be 1486.6 eV. The sample was tilted such that the escape electrons were collected using an electron analyser normal to the sample surface. The circular area of the sample from which escaping electrons were detected was approximately 2 mm in diameter. All spectra were collected in constant analyser energy (CAE) mode at pass energy of 20 eV in 0.5 eV steps between data points. The spectrometer was calibrated with a sputtered copper (99.999% pure) sample, and deposited gold on the sample gave Cu  $2p_{3/2}$ , Cu  $K_{LL}$  and Au  $4f_{7/2}$  binding energies of 932.60 eV, 334.8 eV (kE) and 84.06 eV, respectively. All specimens for analysis in the Microlab were mounted on aluminium stubs using double-sided adhesive conducting carbon tape. The base pressure of the analysis chamber was  $6 \times 10^{-11}$  Torr before specimens were introduced. The binding energies were calibrated with reference to C 1s at 285.0 eV for hydrocarbon contamination.

The oxygen sensing properties of sensors based on the  $\text{Al}_2\text{O}_3\text{-ZrO}_2\text{-Y}_2\text{O}_3$  eutectic composites and polycrystalline zirconia sensors with the same concentration of  $\text{Y}_2\text{O}_3$  dopant were investigated in a conventional gas flow apparatus with heating equipment. The EMF was measured by a computerised multimeter system with high impedance ( $>10$  M $\Omega$ ) (34401A Hewlett-Packard, USA). Certified binary ( $\text{N}_2+\text{O}_2$ ) gas mixtures with different oxygen concentrations were used for oxygen sensing measurements. All tests were carried out using nitrogen as a carrier gas. In all measurements, the airflow rate was  $\sim 100$   $\text{cm}^3/\text{min}$ . The oxygen sensing properties of sensors based on the polycrystalline  $\text{Al}_2\text{O}_3\text{-ZrO}_2\text{-Y}_2\text{O}_3$  solid electrolyte are shown for comparison.

## 3. Results and Discussions

### 3.1 Structure

It has been established that the structure of the shaped  $\text{Al}_2\text{O}_3\text{-ZrO}_2(\text{Y}_2\text{O}_3)$  eutectic composite, as well as the structure of composites obtained by other methods of directional solidification in this system, consists of two phases: the matrix, which is alumina, and stabilised zirconia.<sup>(14)</sup> In this  $\text{Al}_2\text{O}_3\text{-ZrO}_2$  system, alumina is the first phase obtained at growth rates of 20 mm/h and higher. In ref. (14) it was also reported that the microhardness values and fracture toughness of the  $\text{Al}_2\text{O}_3\text{-ZrO}_2(\text{Y}_2\text{O}_3)$  eutectic crystals at a temperature of 20°C are about 1700  $\text{kg}/\text{mm}^2$  and 5.6  $\text{Mpa}\cdot\text{m}^{1/2}$ . Figure 1 shows SEM photographs of the

colony microstructure of  $\text{Al}_2\text{O}_3\text{-ZrO}_2\text{-Y}_2\text{O}_3$  eutectic composites. The  $\text{Al}_2\text{O}_3\text{-ZrO}_2\text{-Y}_2\text{O}_3$  specimens with 8 mol% of  $\text{Y}_2\text{O}_3$  showed uniform grain size distribution of both zirconia and alumina fibres surrounded by some enormous particles of both alumina and zirconia around 5–10  $\mu\text{m}$  in the sub-micrometer scale (Fig. 1(a)). All specimens have zero porosity.

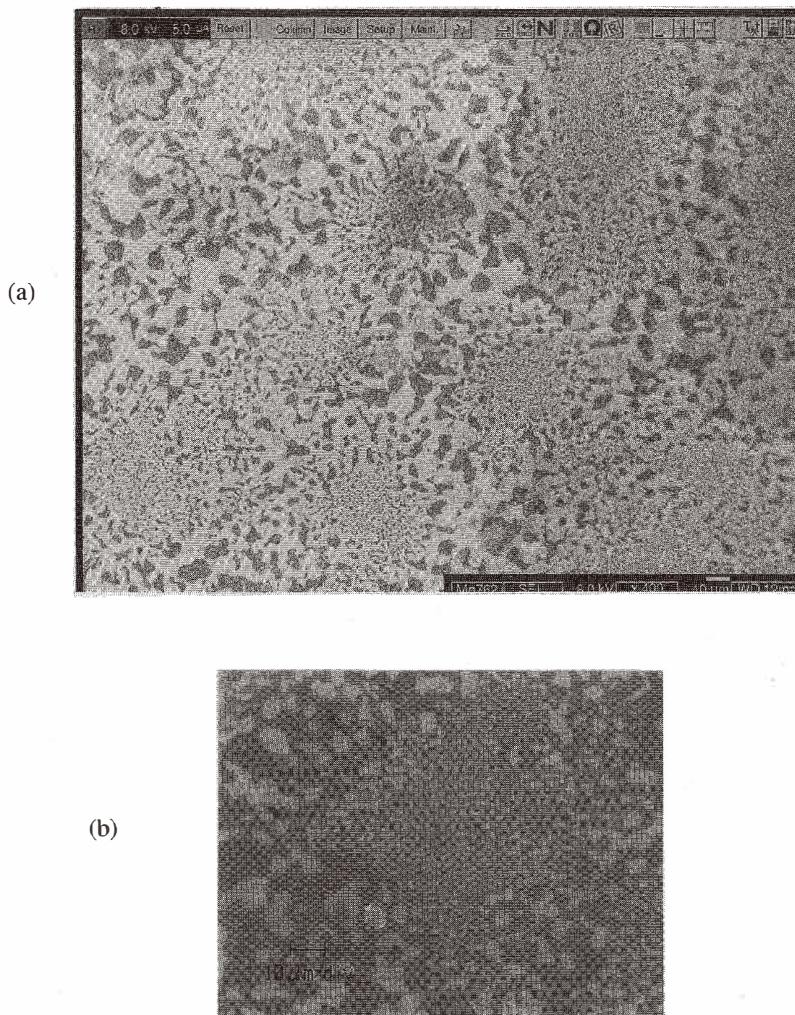


Fig. 1. Typical transverse section of  $\text{Al}_2\text{O}_3\text{-ZrO}_2\text{-Y}_2\text{O}_3$  eutectic composite at different magnifications shown by field emission (SEM). The dark areas are the  $\text{Al}_2\text{O}_3$  phase and the white are the  $\text{ZrO}_2\text{-Y}_2\text{O}_3$  phase: (a) colony structure; and (b) one colony at higher magnification.

The diameter of the  $ZrO_2$  fibres (Fig. 1(b)) in this structure is about 1–2  $\mu m$ . Attainment of a fine, regular structure over the bulk of the crystal and the determination of the growth conditions for which this occurs is one of the main problems in the directional crystallization of eutectic oxide-oxide composites. It is usually assumed that a planar crystallization front is required for the formation of a highly oriented structure in a eutectic system. However, the  $Al_2O_3$ - $ZrO_2$ - $Y_2O_3$  composites displayed the colony structure; the surface of the crystallization front was cellular (Fig. 1(a)). An increase in the growth rate may cause either the faceting of cells or the appearance of dendrites.

In the  $Al_2O_3$ - $ZrO_2$ - $Y_2O_3$  eutectic composites examined here, alumina is the phase, which first grows into the melt. This indicates that with increasing pulling rates, when a condition of supercooling is reached, the alumina matrix becomes faceted at the cellular growth front with part protruding into melt.

Figure 2 shows the microstructure (grain size and porosity distribution) for polished polycrystalline  $Al_2O_3$ - $ZrO_2$ - $Y_2O_3$  specimens at different magnification. The polycrystalline specimens (Fig. 2(a)) showed a uniform grain size distribution with very few isolated

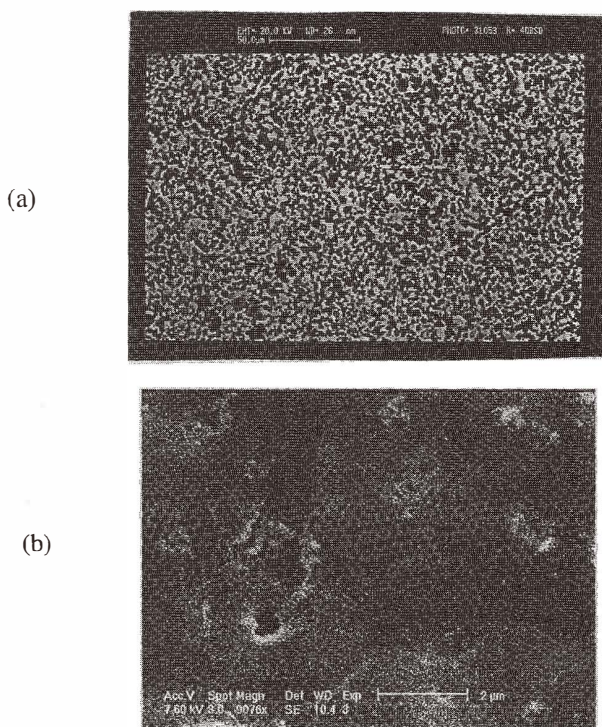


Fig. 2. Scanning electron micrographs recorded from polycrystalline  $Al_2O_3$ - $ZrO_2$ - $Y_2O_3$  specimens showing grain size, porosity and alumina distribution. The dark areas are the  $Al_2O_3$  phase and the white are  $ZrO_2$ - $Y_2O_3$  phase: (a) structure; and (b) structure at higher magnification.

pores (Fig. 2(b)) and the grain size was in the 2.5–6  $\mu\text{m}$  range.

Investigations of the phase assemblage of the eutectic  $\text{Al}_2\text{O}_3\text{-ZrO}_2\text{-Y}_2\text{O}_3$  composites show the presence of mainly two phases, one of which is the phase with the cubic fluorite structure of the  $\text{ZrO}_2\text{-Y}_2\text{O}_3$  composition (Fig. 3(a)). Another phase is alumina (Fig. 3(b)).

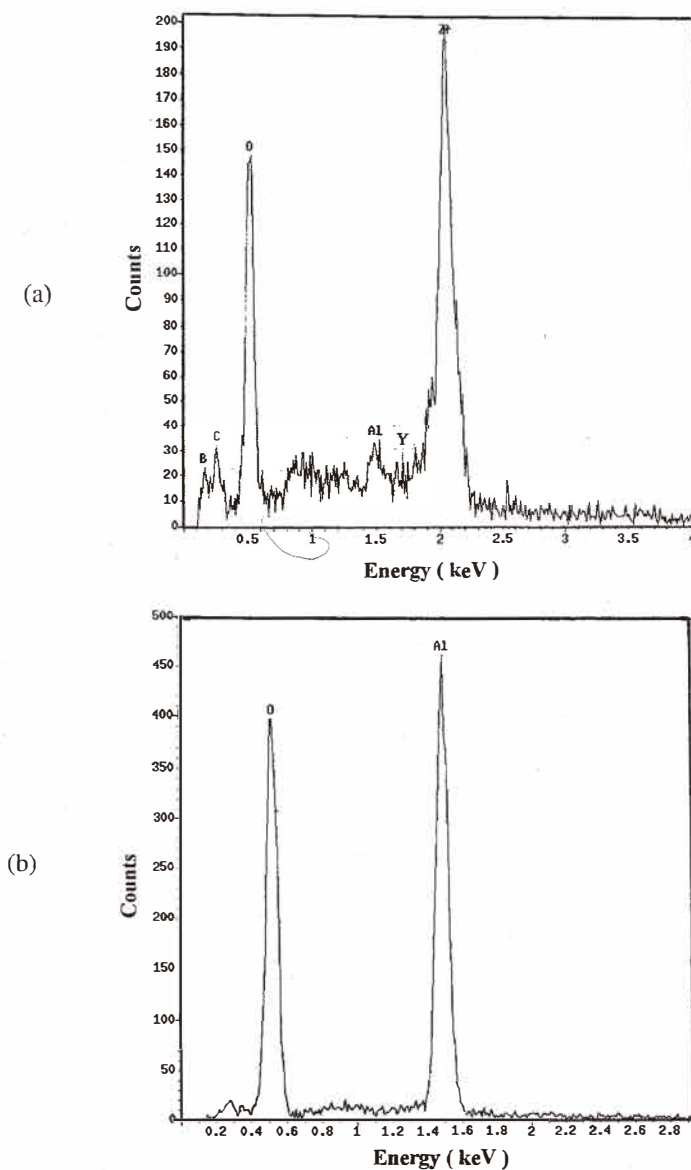


Fig. 3. Energy dispersive X-ray trace of regions of the  $\text{Al}_2\text{O}_3\text{-ZrO}_2\text{-Y}_2\text{O}_3$  crystal: (a) within the grain of the stabilised  $\text{ZrO}_2$ ; and (b) within the grain of  $\text{Al}_2\text{O}_3$ .

Figure 4(a) shows the typical XPS survey spectra for the  $\text{Al}_2\text{O}_3\text{-ZrO}_2\text{-Y}_2\text{O}_3$  composite. It confirms the formation of both the stabilised zirconia with the associated binding energy of the Zr 3d located at 184.16 eV and alumina with associated binding energy of the Al 2p located at 81.40 eV. Photoelectron peaks for Y 3d at 158.67 eV and O 1s at 531.98 eV were also clearly recorded for all specimens. The peaks for Na 1s at 1073.28 eV and for carbon C 1s at 285 eV were detected due to the contamination of the surface of specimens by organic components at the finishing stage of the manufacturing process. However, after

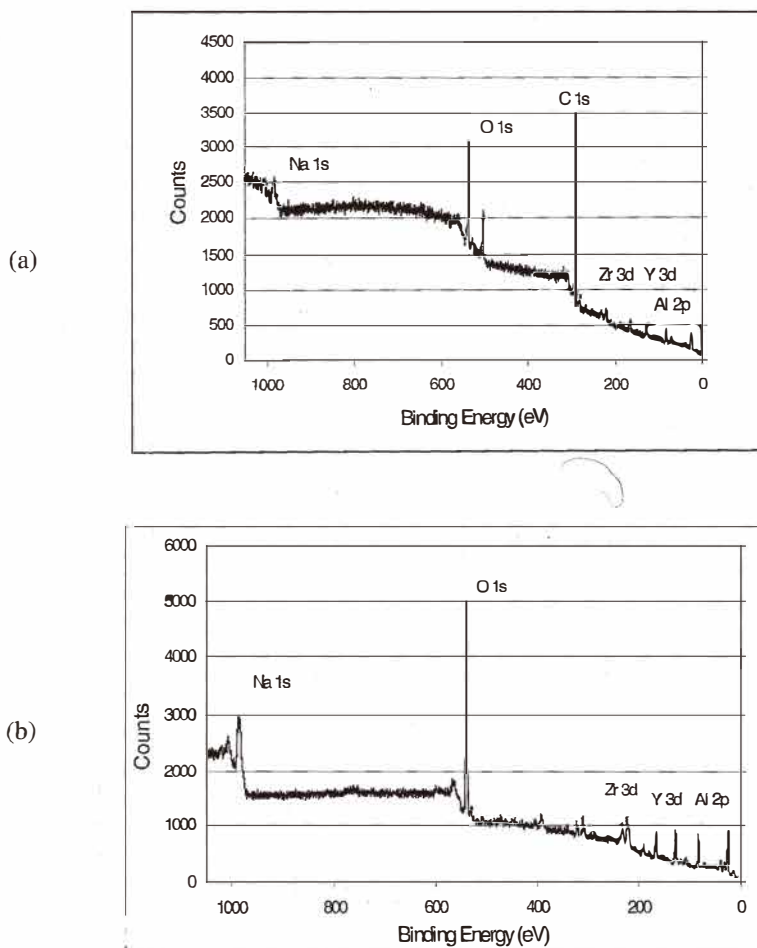


Fig. 4. XPS survey spectra of the surface of  $\text{Al}_2\text{O}_3\text{-ZrO}_2\text{-Y}_2\text{O}_3$  specimens.



cleaning the surface of the  $\text{Al}_2\text{O}_3\text{-ZrO}_2(\text{Y}_2\text{O}_3)$  eutectic composite with neutral gas, the carbon peak disappeared from the survey spectra (Fig. 4(b)). Figures 5(a), 5(b) and 5(c) show high-resolution XPS spectra for Al 2p, Zr 3d and O 1s, respectively. Table 1 summarises the chemical composition of samples calculated from the experimental data in Figs. 5(a), 5(b) and 5(c). The calculation is based on the integrated area under the assigned element peak and the sensitivity factor for the element.<sup>(17)</sup>

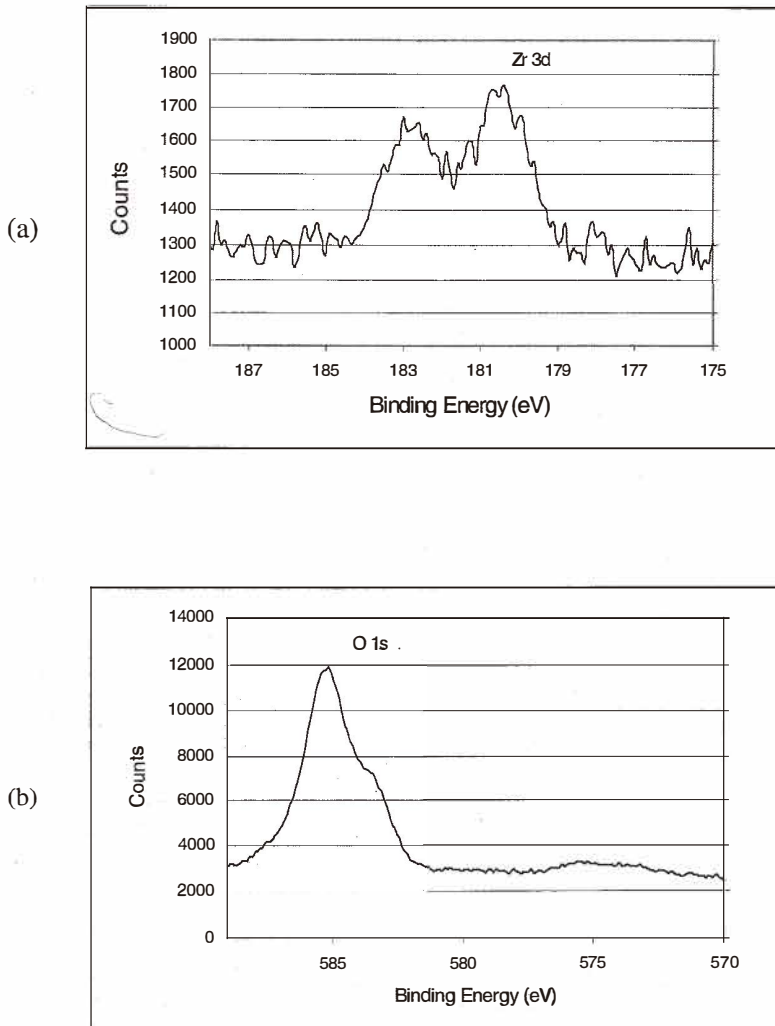


Fig. 5. Typical high-resolution spectra for: (a) Zr 3d; and (b) O 1s.

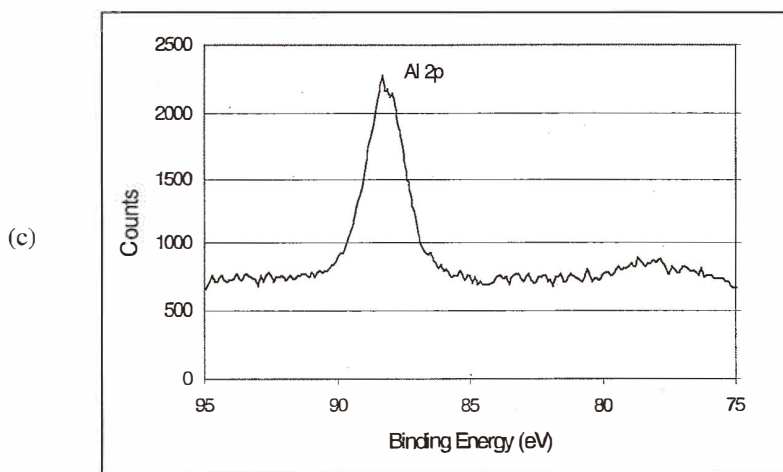


Fig. 5. Typical high resolution spectra for: (c) Al 2p.

Table 1

Chemical composition of the  $\text{Al}_2\text{O}_3\text{-ZrO}_2\text{-Y}_2\text{O}_3$  eutectic composite.

Peak	Centre (eV)	SF	PeakArea	Tx.Function	NormArea	[AC] %
O 1s	531.98	2.93	65045.837	0.1	2537.88621	63.999
Zr 3d	184.16	7.04	14759.895	0.1	193.28330	15.986
Y 3d	158.67	5.98	7907.681	0.1	144.02052	4.018
Al 2p	81.40	0.54	5155.539	0.1	189.56924	15.997

The peak at 531.98 eV is characteristic of metallic oxides and is in agreement with the O 1s electron binding energy for  $\text{ZrO}_2$  and  $\text{Al}_2\text{O}_3$ . From the calculated atomic percentages of Al and Zr it can be seen that the implied oxygen content of  $\text{Al}_2\text{O}_3$  and  $\text{ZrO}_2$  is approximately correct for all samples.

### 3.2 Characteristics of the $\text{Al}_2\text{O}_3\text{-ZrO}_2\text{-Y}_2\text{O}_3$ -based oxygen sensors

Sensors based on the polycrystalline zirconia and sensors based on the  $\text{Al}_2\text{O}_3\text{-ZrO}_2\text{-Y}_2\text{O}_3$  eutectic composite with the same concentration of  $\text{Y}_2\text{O}_3$  dopant were used for resistance measurements at temperatures from 400°C to 800°C. The temperature of the sensors was measured to  $\pm 0.5^\circ\text{C}$  by a K-type thermocouple placed adjacent to the reference electrode. Dry air was used for both electrodes in these tests (20.9% of oxygen). The measured resistance of both sensors was reproducible during heating and cooling cycles. The results of testing are shown in Fig. 6. The lines are approximately parallel, *i.e.*, the samples have similar activation energies. However, the difference in resistance between the eutectic composite and polycrystalline zirconia at temperatures lower than 500°C is

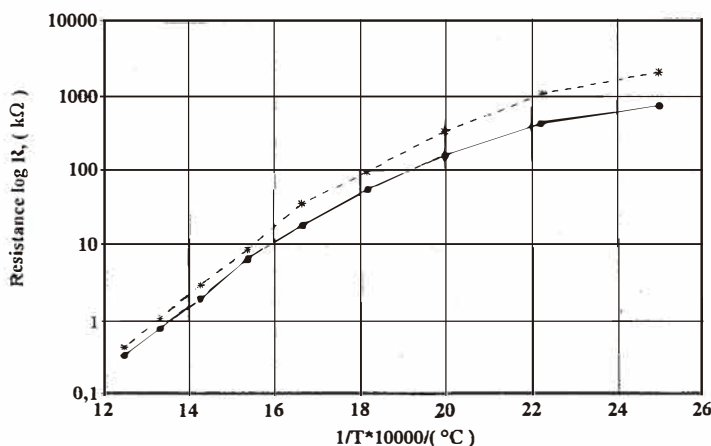


Fig. 6. Temperature dependence of the logarithm of resistance of the zirconia solid electrolyte: (\*) polycrystalline  $\text{Al}_2\text{O}_3\text{-ZrO}_2\text{-Y}_2\text{O}_3$ ; (•)  $\text{Al}_2\text{O}_3\text{-ZrO}_2\text{-Y}_2\text{O}$  eutectic crystal.

still significant, probably due to the affect of impurities in the polycrystalline ceramic.

To find the lowest possible temperature at which the output EMF of a sensor based on an eutectic composite closely followed the Nernst equation, experiments were performed in the operating temperature range of 450°C to 600°C. Dry air was used as a reference gas. A  $\text{N}_2+\text{O}_2$  mixture with 100 ppm of oxygen was used as a measuring gas. The airflow rate on the measuring electrode was equal to the airflow rate on the reference electrode and was  $\sim 100 \text{ cm}^3/\text{min}$  to avoid polarization on electrodes. Furthermore, to avoid the thermoelectric effect on electrodes, it was necessary to maintain the airflow rate constant for both electrodes. The electrode electrochemical reactions at this temperature range have low rate. The steady state EMFs were obtained after only 5–6 min for the sensor based on the  $\text{Al}_2\text{O}_3\text{-ZrO}_2\text{-Y}_2\text{O}_3$  eutectic composite. Each EMF measurement was reversible and was made after each change of temperature. As reported previously,<sup>(4)</sup> the steady state EMF for the polycrystalline zirconia sensor with  $(\text{U,Sc})\text{O}_{2+x} + \text{Pt}$  electrodes were obtained after about 15–20<sup>(5)</sup> min for the same temperature range. Tests were conducted for several heating and cooling cycles. Figure 7 shows the temperature dependence of an average ionic transference number ( $\bar{t}_{\text{ion}} = \text{EMF}_{\text{exp.}} / \text{EMF}_{\text{theory}}$ ) calculated for a sensor based on the  $\text{Al}_2\text{O}_3\text{-ZrO}_2\text{-Y}_2\text{O}_3$  eutectic composite. The  $\bar{t}_{\text{ion}}$  numbers at the same temperatures for both  $\text{Al}_2\text{O}_3\text{-ZrO}_2\text{-Y}_2\text{O}_3$  and  $\text{Al}_2\text{O}_3\text{-ZrO}_2\text{-Sc}_2\text{O}_3$  polycrystalline electrolyte sensors with Pt and  $(\text{U,Sc})\text{O}_{2+x} + \text{Pt}$  electrodes<sup>(4,6)</sup> are presented for comparison. In these results the Pt content in the  $(\text{U,Sc})\text{O}_{2+x} + \text{Pt}$  electrodes was from 40 wt% to 75 wt%.<sup>(4)</sup> The complex nature of the  $(\text{U,Sc})\text{O}_{2+x} + \text{Pt}$  electrode allows it to trap the oxygen molecules on the  $(\text{U,Sc})\text{O}_{2+x}$  oxides and to enhance the catalytic activity of the Pt on the triple line to dissociate the oxygen molecules on ions at the low temperatures. Pt, as an electrode material, cannot itself adequately promote the oxygen dissociation on ions at this temperature range.

As the operating temperature increased, the Nernstian behaviour of the sensor based on

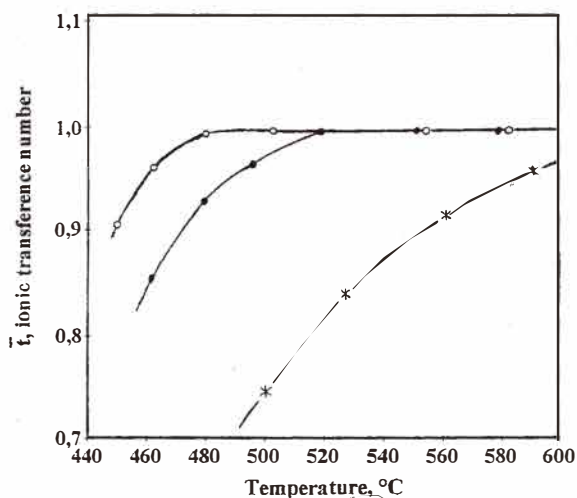


Fig. 7. The temperature dependence of an average ionic transference number for zirconia solid electrolytes: (\*) polycrystalline  $\text{Al}_2\text{O}_3\text{-ZrO}_2\text{-Y}_2\text{O}_3$  ceramic with Pt electrodes; (●) polycrystalline  $\text{Al}_2\text{O}_3\text{-ZrO}_2\text{-Sc}_2\text{O}_3$  with  $(\text{U, Sc})\text{O}_{2+x}$  + Pt electrodes; (°)  $\text{Al}_2\text{O}_3\text{-ZrO}_2\text{-Y}_2\text{O}_3$  composite eutectic crystals.

$\text{Al}_2\text{O}_3\text{-ZrO}_2\text{-Y}_2\text{O}_3$  eutectic became more predominant. The reproducibility of the measured EMF at temperatures higher than  $480^\circ\text{C}$  was reasonably good ( $\pm 1$  mV). The low value of the output EMF for the polycrystalline zirconia sensors at operating temperatures less than  $500^\circ\text{C}$  can be explained by the absence of electrochemical equilibrium on the electrodes. The rate of the reaction between electrolyte-electrode and gas phases is generally small at low temperatures. This rate increases with temperature. In comparison with other polycrystalline sensors, the sensor based on  $\text{Al}_2\text{O}_3\text{-ZrO}_2\text{-Y}_2\text{O}_3$  eutectic composite with Pt electrodes exhibited a good output stability even at the temperature of  $480^\circ\text{C}$ . For a similar sensor based on  $\text{Al}_2\text{O}_3\text{-ZrO}_2\text{-Sc}_2\text{O}_3$  ceramic with  $(\text{U, Sc})\text{O}_{2+x}$  + Pt electrodes, the response at the same temperature requires much longer time ( $\sim 10 - 20$  minutes),<sup>(5)</sup> which is unsatisfactory for industrial applications. Further, the  $(\text{U, Sc})\text{O}_{2+x}$  + Pt electrodes adhere poorly to the solid electrolyte and come off easily after relatively short periods of time. Thus, the sensor based on  $\text{Al}_2\text{O}_3\text{-ZrO}_2\text{-Y}_2\text{O}_3$  eutectic composite with Pt electrodes could be used as an alternative oxygen sensor at temperatures as low as  $480^\circ\text{C}$ .

Figure 8 shows the response and recovery times of the sensor based on  $\text{Al}_2\text{O}_3\text{-ZrO}_2\text{-Y}_2\text{O}_3$  eutectic composite with Pt electrodes. The 90% response time was only 55 sec upon exposure to gas containing 1000 ppm  $\text{O}_2$  at  $500^\circ\text{C}$ . The recovery time was also rapid. However, the EMF returned to its original level within  $\sim 100$  sec. Although this sensor has much faster response and recovery at high temperatures (less than 1 sec at temperatures above  $700^\circ\text{C}$ ), it almost satisfies the response characteristics demanded for practical

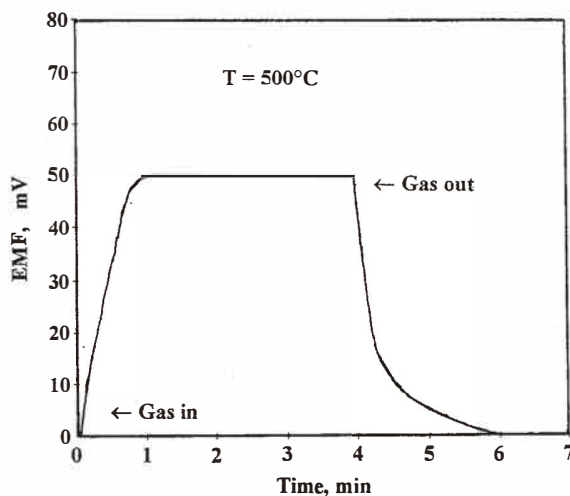


Fig. 8. The response and recovery times of the oxygen sensor based on the  $\text{Al}_2\text{O}_3\text{-ZrO}_2\text{-Y}_2\text{O}_3$  eutectic composites.

sensors working at the temperature range of 450°C to 600°C.<sup>(18)</sup> Numerous measurements of different  $\text{O}_2$  concentrations at this temperature range have been shown that the sensor EMF values agree almost linearly with the logarithm of oxygen concentration from 0.1 ppm up to 100 %. The main sensor characteristics of both  $\text{Al}_2\text{O}_3\text{-ZrO}_2\text{-Y}_2\text{O}_3$  eutectic composite with Pt electrodes and  $\text{Al}_2\text{O}_3\text{-ZrO}_2\text{-Sc}_2\text{O}_3$  electrolyte with  $(\text{U,Sc})\text{O}_{2+x}$  + Pt electrodes at temperatures higher than 550°C did not differ significantly. Furthermore, continuous oxygen measurements at an operating temperature range of 550°C to 1000°C show that the sensors based on  $\text{Al}_2\text{O}_3\text{-ZrO}_2\text{-Y}_2\text{O}_3$  eutectic composite with Pt electrodes accurately measure oxygen not only at low but also at high temperatures. The measured EMF closely followed the Nernst equation ( $\pm 1$  mV) in the working temperature range of 600°C to 1000°C. Figure 9 shows the EMF of the sensor based on  $\text{Al}_2\text{O}_3\text{-ZrO}_2\text{-Y}_2\text{O}_3$  eutectic composite with the air reference electrode as a function of measuring temperature at different oxygen concentrations. There is a strong correlation between the test results and the calculated EMF from the Nernst equation in both the high-temperature and low-temperature regimes. This implies that the sensors based on  $\text{Al}_2\text{O}_3\text{-ZrO}_2\text{-Y}_2\text{O}_3$  eutectic composite can measure successfully the oxygen concentration from 0.1 ppm not only at low temperatures, but also at high temperatures.

Above 700°C, the values of response time for the sensor are limited by the inherent speed of the electronic measuring equipment. True response times are probably less than those shown. It can be seen that the response time of the high temperature sensor is ~ 130 ms or less<sup>(4)</sup> over its normal temperature range, whereas the values of response time exceeded one minute as a typical response of the zirconia sensor below 400°C.<sup>(13)</sup>

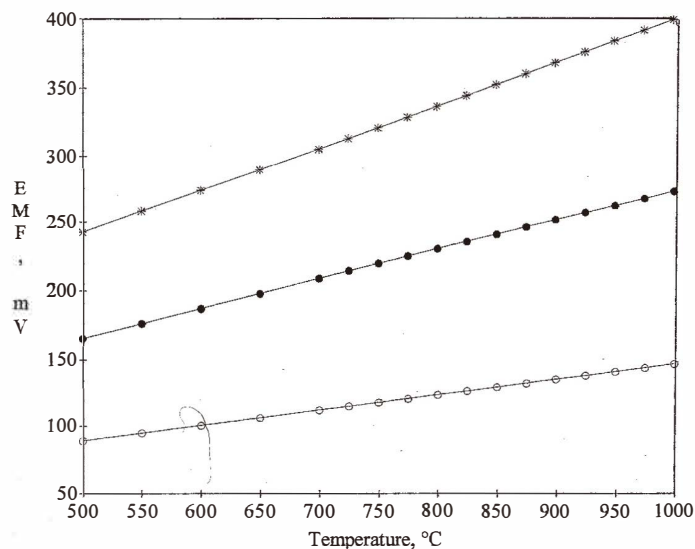


Fig. 9. Correlation between the Nerstian (line) and measured (symbol) EMF for the sensor based on  $\text{Al}_2\text{O}_3\text{-ZrO}_2\text{-Y}_2\text{O}_3$  eutectic composite with Pt electrodes at different oxygen concentrations: (\*) 0.1 ppm; (●) 10 ppm; and (°) 10000 ppm.

Several important features about the influence of airflow rate on the EMF measurements are worth reporting. At temperatures less than  $530^\circ\text{C}$ , the airflow rate of more than  $100\text{ cm}^3/\text{min}$  has a cooling effect on the electrodes. In this case the electrode reactions at the electrode/electrolyte interface are sluggish. Furthermore, if airflow rate at the reference electrode differs significantly from the airflow rate at the measuring electrode, it may result in a thermoelectric effect on the electrodes. As a consequence of this, EMF mismeasurements occur. Therefore, the airflow rate for the solid electrolyte sensors working at a temperature range of  $480^\circ\text{C}$  to  $530^\circ\text{C}$  should not be higher than  $100\text{ cm}^3/\text{min}$ . At temperatures higher than  $530^\circ\text{C}$ , the influence of the airflow rate on the EMF measurements is negligible.

Thus, the sensors based on  $\text{Al}_2\text{O}_3\text{-ZrO}_2\text{-Y}_2\text{O}_3$  eutectic composite with Pt electrodes appear to have a high level of reliability and long-term chemical stability and can be used not only for oxygen measurement at low temperatures but also for the oxygen measurement at high temperatures in gaseous and possibly molten metal environments. The output EMFs obtained from these sensors were constant and reproducible from cycle to cycle over a large number of tests.

#### 4. Conclusions

The purpose of this investigation was to study the structural and gas sensing properties of  $\text{Al}_2\text{O}_3\text{-ZrO}_2\text{-Y}_2\text{O}_3$  eutectic composites. The results obtained suggest that the composites have a colony structure; the surface of the crystallization front is cellular. Results also indicate that when the direction of composite growth is parallel to [001], the cells are faceted by rhombohedral planes and alumina is the phase, which first grows into the melt. The XPS results summarise the morphology, crystalline structure and chemical composition of the  $\text{Al}_2\text{O}_3\text{-ZrO}_2\text{-Y}_2\text{O}_3$ -shaped eutectic composite. Carbon was the dominant impurity at the surface of the composite. The investigation of the sensors based on  $\text{Al}_2\text{O}_3\text{-ZrO}_2\text{-Y}_2\text{O}_3$  eutectic composite with Pt electrodes provides evidence that these composites behave as pure ionic conductors at temperatures as low as  $480^\circ\text{C}$ . These findings indirectly confirm the conclusions about the superior ionic conductivity of the zirconia single crystals with Pt electrodes,<sup>(13)</sup> which appears only at temperatures  $T \geq 480^\circ\text{C}$ . Comparison of the results obtained for the sensors based on  $\text{Al}_2\text{O}_3\text{-ZrO}_2\text{-Y}_2\text{O}_3$  eutectic composite with the results obtained for the sensors based on polycrystalline  $\text{Al}_2\text{O}_3\text{-ZrO}_2\text{-Y}_2\text{O}_3$  electrolyte and previous results for sensors based on polycrystalline zirconia with  $\text{Sc}_2\text{O}_3$  dopant and  $(\text{U,Sc})\text{O}_{2+x}$  + Pt electrodes showed that the  $\text{Al}_2\text{O}_3\text{-ZrO}_2\text{-Y}_2\text{O}_3$  eutectic composites appear to be more effective than polycrystalline ceramics in promoting oxygen transfer at the operating temperature range of  $480^\circ\text{C}$  to  $550^\circ\text{C}$  and are also less affected by higher temperature exposure.

#### Acknowledgments

The author thanks Professor N. Yamazoe and Mr. T. Kida (Department of Molecular and Materials Science, Kyushu University) for their valuable support in preparation of SEM and XRD tests. The author also thanks Professor N. Miura for valuable discussions.

#### References

- 1 P. S. Manning, J. D. Sirman, R. A. De Souza and J. A. Kilner: *Solid State Ionics* **100** (1997) 1.
- 2 S. Zhuiykov: *J. Europ. Cer. Soc.* **20** No.7 (2000) 967.
- 3 A. Ziehfrend, U. Simon and W. F. Maier: *Adv. Mater.* **8** No.5 (1997) 424.
- 4 S. P. S. Badwal, M. J. Banister and W. G. Garrett: *J. Phys. E: Sci. Instrum.* **20** (1987) 531.
- 5 S. P. S. Badwal and F. T. Ciacchi: *J. Appl. Electrochem.* **16** (1986) 28.
- 6 S. P. S. Badwal: *J. Electrochem. Soc.* **14** (1984) 379.
- 7 S. P. S. Badwal, F. T. Ciacchi, S. Rajendran and J. Drennan: *Solid State Ionics* **109** (1998) 167.
- 8 D. J. M. Burhard, B. Hanson and G. C. Ulmer: *Solid State Ionics* **47** (1991) 169.
- 9 J. Nowotny and C. C. Sorrell: *Electrical Properties of Oxide Materials* (Trans. Tech., Switzerland, 1997).
- 10 W. Wepner and H. Schubert: *Advances in Ceramics, Science & Technology of Zirconia* **24** (1988) 725.
- 11 S. Zhuiykov, P. Talanchuk and B. A. Shmatko: *Herald Kiev Pol. Ins.: Instrumentation* **22** (1992) 49.
- 12 Z. Y. Can, H. Narita, J. Mizusaki and H. Tagawa: *Solid State Ionics* **79** (1995) 344.

- 13 S. Zhuiykov: *Process Control & Quality* **11**, No.1 (1998) 23.
- 14 V. A. Borodin, M. Y. Starostin and T. N. Yalovets: *J. of Crystal Growth* **104** (1990) 148.
- 15 S. P. S. Badwal: *J. Appl. Electrochem.* **14** (1984) 379.
- 16 S. Zhuiykov, H. Kanost and A. Walker: Australian Patent No. **693,735** (1998).
- 17 J. F. Moulder, W. F. Stickle, P. E. Sool and K. D. Bomben, *Handbook of X-ray Photoelectron Spectroscopy*, Perkin-Elmer, Eden Pizirie, 1992.
- 18 A. M. Azad, S. A. Akbar, S. G. Mhaisalkar, L. D. Birkefeld and K. S. Goto: *J. Electrochem. Soc.* **139**, No.12 (1992) 3690.



**Dr. Serge Zhuiykov** was awarded a Ph.D in Materials Science and Technology at The Ukrainian State Technical University, Kiev, Ukraine in 1991. From 1991 to 1994 he was a Research Scientist at the above-mentioned University. From 1994 to 1998 he was appointed as a Research Scientist at Ceramic Oxide Fabricators Pty. Ltd., Australia. From 1999 to 2000 he was working as a Research Scientist at the Royal Melbourne Institute of Technology, Melbourne, Australia. He developed the semiconductor oxygen sensors for combustion and the solid electrolyte O<sub>2</sub>, SO<sub>x</sub>, CO and H<sub>2</sub> sensors for different applications including oxygen sensors for molten metals. He has published over 30 papers and

holds 13 patents. He was selected as a recipient of the Australasian Ceramic Society/ Ceramic Society of Japan Joint Award for Young Distinguished Scientist in 1998. His current research interests include the development of semiconductor and solid electrolyte gas sensors, sensor design and thin-film manufacturing technologies. Dr. Zhuiykov is currently working as a Postdoctoral Fellow at the Advanced Science & Technology Center for Cooperative Research at Kyushu University, Japan.